Molecular Cell
Article

The Autophagy Protein Atg12 Associates with Antiapoptotic Bcl-2 Family Members to Promote Mitochondrial Apoptosis

Assaf D. Rubinstein,[1] Miriam Eisenstein,[2] Yaara Ber,[1] Shani Bialik,[1] and Adi Kimchi[1,*]
[1]Department of Molecular Genetics
[2]Department of Chemical Research Support
Weizmann Institute of Science, Rehovot 76100, Israel
*Correspondence: adi.kimchi@weizmann.ac.il
DOI 10.1016/j.molcel.2011.10.014

SUMMARY

Autophagy and apoptosis constitute important determinants of cell fate and engage in a complex interplay in both physiological and pathological settings. The molecular basis of this crosstalk is poorly understood and relies, in part, on "dual-function" proteins that operate in both processes. Here, we identify the essential autophagy protein Atg12 as a positive mediator of mitochondrial apoptosis and show that Atg12 directly regulates the apoptotic pathway by binding and inactivating prosurvival Bcl-2 family members, including Bcl-2 and Mcl-1. The binding occurs independently of Atg5 or Atg3 and requires a unique BH3-like motif in Atg12, characterized by interaction studies and computational docking. In apoptotic cells, knockdown of Atg12 inhibited Bax activation and cytochrome c release, while ectopic expression of Atg12 antagonized the antiapoptotic activity of Mcl-1. The interaction between Atg12 and Bcl-2 family members may thus constitute an important point of convergence between autophagy and apoptosis in response to specific signals.

INTRODUCTION

Autophagy is an evolutionarily conserved catabolic process in which cytoplasmic proteins and organelles are engulfed within de novo formed double-membrane vesicles (termed autophagosomes) and delivered to lysosomes for degradation and recycling. Autophagy promotes cell survival by clearance of damaged organelles and aggregate-prone proteins, elimination of intracellular pathogens, and recycling of essential macromolecules during periods of nutrient limitation (Levine and Kroemer, 2008). In specific cases, autophagy may also serve as a nonapoptotic form of programmed cell death through excessive self-consumption and/or selective degradation of prosurvival factors (Berry and Baehrecke, 2007; Denton et al., 2009; Gozuacik et al., 2008).

Autophagy is governed by a set of autophagy-related (*Atg*) genes that operate concertedly during the process of autophagosome biogenesis (Yang and Klionsky, 2010). Autophagy requires the function of two ubiquitin-like processes, which catalyze the covalent conjugation of Atg12 to Atg5 and of MAP1-LC3 (the mammalian ortholog of yeast Atg8) to the lipid phosphatidylethanolamine (PE) (Tanida et al., 2004). These reactions are facilitated by a common E1-like enzyme, Atg7, and by specific E2-like enzymes, Atg3 and Atg10, which subsequently catalyze the conjugation of LC3 to PE and of Atg5 to the C-terminal glycine of Atg12, respectively. Finally, the Atg5-Atg12 conjugate proceeds to form an active multimeric complex together with Atg16 that localizes to sites of autophagosome assembly (Kuma et al., 2002). Recently, Atg3 was reported as an additional conjugation partner of Atg12 (Radoshevich et al., 2010). Interestingly, conjugation of Atg12 to Atg3 serves to regulate mitochondrial homeostasis and cell death, without an apparent role in autophagy.

Whether promoting cell survival or cell death, autophagy is intimately linked with apoptosis, and the two processes engage in a complex and poorly understood molecular crosstalk (Eisenberg-Lerner et al., 2009; Maiuri et al., 2007b). One level of crosstalk involves the utilization of common proteins that regulate both apoptosis and autophagy. For example, pro- and antiapoptotic members of the Bcl-2 family regulate autophagy in addition to their canonical function in controlling the intrinsic pathways of caspase activation. Bcl-2 and related antiapoptotic family members suppress autophagy by binding to the Bcl-2 homology 3 (BH3) domain of Beclin-1, an essential component of the class III PI3K/Vps34 complex that is necessary for autophagy induction (Erlich et al., 2007; Germain et al., 2011; Pattingre et al., 2005; Sinha and Levine, 2008). Conversely, proapoptotic "BH3-only" proteins promote autophagy by disrupting the Bcl-2-Beclin-1 interaction (Maiuri et al., 2007a). More recently, data from several studies suggested that the interplay between autophagy and apoptosis also extends to "core machinery" proteins, which double as essential components of one pathway and regulators of the other. Examples of such "dual-function" proteins include the apoptotic caspases, which suppress autophagy through cleavage of Beclin-1 and Vps34 (Cho et al., 2009; Luo and Rubinsztein, 2010; Zhu et al., 2010), and Atg5, which has apoptotic roles that are separate from its function in autophagy (Pyo et al., 2005; Yousefi et al., 2006; Zalckvar et al., 2010).

In this work, we sought to expand the view of this important facet of the crosstalk between autophagy and apoptosis by identifying additional components of the autophagic machinery that double as positive mediators of apoptosis. Through RNAi screening of mammalian autophagy genes, we identified Atg12 as an essential regulator of mitochondrial apoptosis induced by several stimuli. We found that the apoptotic function of Atg12 is mediated by a previously unknown interaction with antiapoptotic members of the Bcl-2 family that results in their inactivation. In addition, we identified a BH3-like motif in Atg12 that is required for binding to Bcl-2 proteins, and we present a possible structural model for the interaction based on in silico homology modeling and protein-protein docking.

RESULTS

RNAi Screen Identifies Atg12 as a Positive Mediator of Apoptosis

To identify individual autophagic genes that function as positive mediators of apoptosis, a library of siRNA pools targeting most of the known mammalian autophagy genes was screened. To this end, HEK293 cells were reverse-transfected with the appropriate siRNAs (siGENOME; Dharmacon) 24 hr prior to application of the apoptotic stimulus. Cells were then exposed to the DNA-damaging drug etoposide for a period of 48 hr, and the extent of apoptosis was determined by measuring the activity of caspase-3 and caspase-7 using a luciferase-based caspase activity assay. The screen was performed in three independent biological replicates, each containing three technical replicates per siRNA. Positive mediators of apoptosis were defined as genes whose knockdown led to significant attenuation of caspase-3/7 activity compared to nontargeting controls in all three biological repeats of the screen.

Data obtained from the three biological replicates of the screen exhibited a high degree of correlation (Figure S1A). Analysis of the screen results according to autophagic gene families revealed that while some families exhibited uniform behavior, others displayed marked variability in the effect of individual family members on caspase activity (Figure 1A). For example, knockdown of five out of the six mammalian orthologs of Atg8 (LC3B, LC3C, GABARAP, GABARAPL1,2) led to a moderate decrease in caspase activity, raising the possibility that these proteins may share a similar, and perhaps not fully redundant, function in apoptosis. In contrast to the Atg8 family, the four orthologs of the protease Atg4 (Atg4A-D) displayed substantial variability in their effect on caspase activity, with Atg4A and Atg4C/D having opposite effects. These initial observations require further validation in order to fully elucidate the possible involvement of these gene families in apoptosis. Nevertheless, the finding that some autophagic genes inhibited caspase activity while others stimulated caspase activity or had no effect, indicates that the observed effects are most likely a result of independent functions of specific autophagy genes in their crosstalk with the apoptosis pathway, rather than a global effect of autophagy inhibition on cell death.

The most pronounced effect, however, was observed upon knockdown of the essential autophagy gene *Atg12,* which led to a marked inhibition of caspase activity (Figure 1A and Table S1) ($p < 0.0001$). The depletion of Atg12 was distinct from other autophagy genes, which exhibited milder effects on caspase activity, suggesting that Atg12 was essential for effective progression of apoptosis induced by DNA damage. Similar results were obtained when activation of caspase-3 and caspase-7 was evaluated by western blot analysis under similar conditions. As shown in Figure 1B, both the processing of caspase-3 and caspase-7 to their active forms, as well as cleavage of their downstream target PARP-1, were attenuated in response to knockdown of Atg12 in etoposide-treated cells.

Parallel measurements of DNA content per well indicated that cell number did not vary between Atg12-depleted cells and control siRNA-transfected cells, excluding possible false positive effects due to reduced cell number (Figure S1B). To address the possibility of off-target effects, the results of the screen were validated by knocking down Atg12 with chemically modified ON-TARGET*plus* (OTP) siRNA (Jackson et al., 2006), with results similar to the original screen (Figure S1C). Further validation was carried out by depletion of Atg12, using five individual siRNA duplexes. All five siRNAs led to a significant attenuation of effector caspase activity in response to etoposide treatment (Figure S1D).

To verify that the apoptotic function of Atg12 was not limited to a specific cell type or trigger, the effect of Atg12 depletion was examined in additional cell types and with several different inducers of apoptosis (Figure 1C). Reduced activity of caspase-3/7 was observed upon knockdown of Atg12 in HeLa cells treated with staurosporine (STS), paclitaxel (taxol), TNF-α, etoposide, or tunicamycin and in A549 cells treated with STS, C_6-ceramide, or etoposide. Knockdown of caspase-3 served as a positive control in these experiments. Notably, the results were reproduced with a second siRNA duplex targeting Atg12 (data not shown). In contrast, depletion of Atg12 had little effect on caspase activation by CD-95 agonistic antibody in the type-I cell lines ACHN (Figure 1D) and HepG2 (data not shown). In these cells, Fas-induced apoptosis proceeds via the mitochondria-independent pathways of extrinsic apoptosis (Barnhart et al., 2004). Thus, Atg12 is implicated specifically in apoptotic pathways that converge on mitochondria.

Because the pan-kinase inhibitor STS induces rapid activation of mitochondrial apoptosis, as opposed to other triggers which also activate complex cellular responses, such as the DNA damage response or the ER stress response, this trigger was further analyzed in depth. In STS-treated HeLa cells, the attenuation of caspase-3 by Atg12 depletion was accompanied by a decrease in cleavage of its direct downstream substrates, ICAD and PARP-1 (Figure 2A). At the cellular level, Atg12-depleted cells exhibited decreased morphological signs of nuclear fragmentation, a hallmark of apoptotic cell death (Figure 2B). More importantly, the impairment in caspase activation upon loss of Atg12 also correlated with decreased susceptibility to STS-induced cell death, as assessed by plasma membrane integrity (Figure 2C), metabolic capacity (Figure 2D), and clonogenic survival (Figure 2E). Increased viability of Atg12-depleted cells was likewise observed with several other apoptotic triggers and cell lines (Figure S2).

Atg12 Associates with Antiapoptotic Bcl-2 Family Members via a BH3-like Motif

We reasoned that one possible way by which Atg12 could regulate apoptosis is via direct interaction with components of the

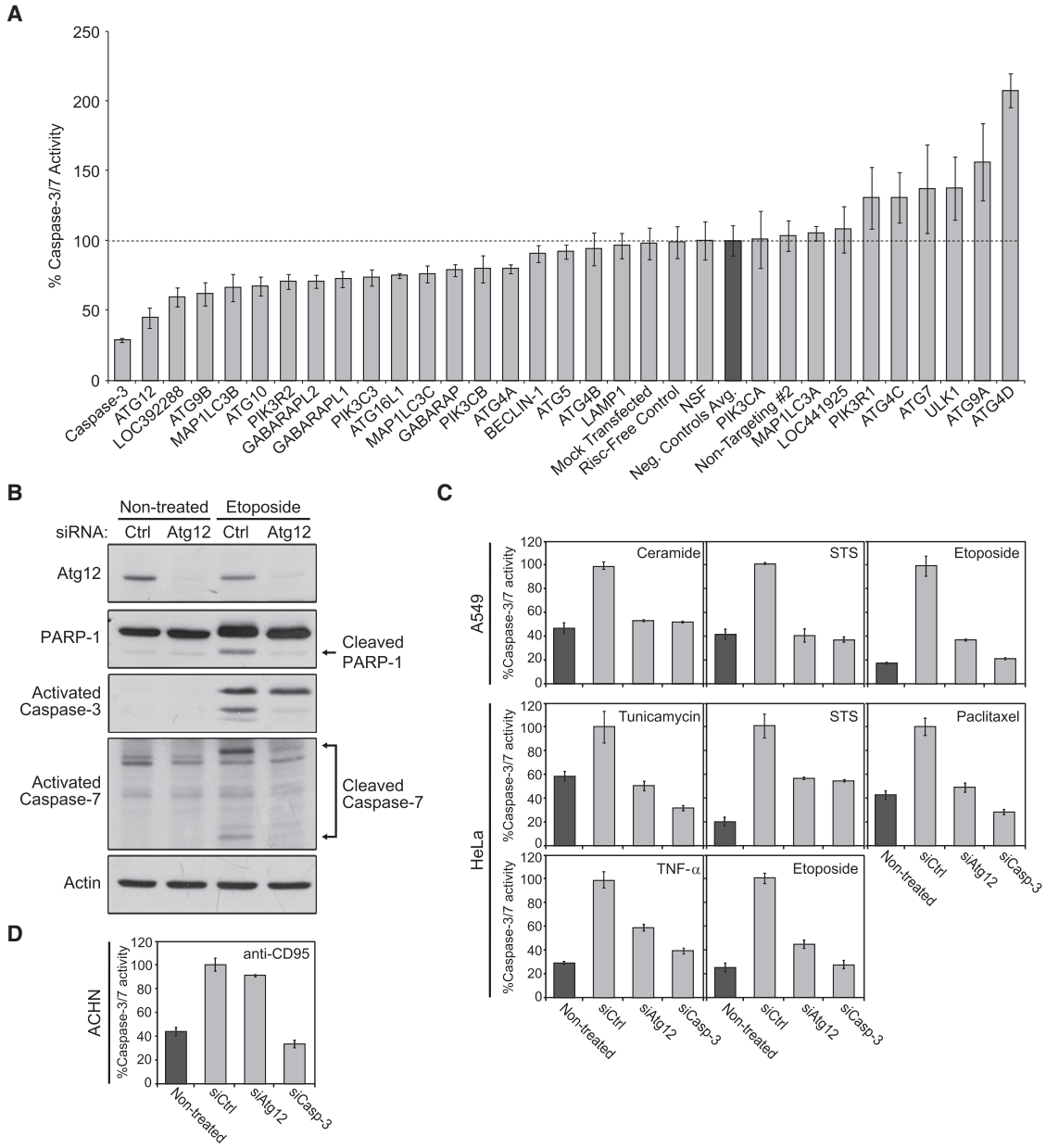

Figure 1. An siRNA-Based Screen of Mammalian Autophagy Genes Identifies Atg12 as a Positive Mediator of Apoptosis

(A) HEK293 cells transfected with the indicated siRNA pools were treated with 50 μM etoposide for 48 hr. For each gene, levels of caspase-3/7 activity relative to the average of three nontargeting controls were determined using the Caspase-Glo 3/7 assay. Results represent mean ± SD of combined data from three independent screens.

(B) HEK293 cells transfected with the indicated siRNA pools were treated with 50 μM etoposide for 48 hr and subjected to western blot analysis for molecular markers of apoptosis.

(C) Caspase-3/7 activity (mean ± SD) relative to nontargeting siRNA pool in HeLa cells treated with STS (2 μM; 4 hr), paclitaxel (10 μM; 24 hr), etoposide (100 μM; 24 hr), TNF-α/CHX (60 ng/ml; 6 hr), and tunicamycin (1.5 μg/ml; 24 hr); and in A549 cells treated with C_6-ceramide (50 μM; 24 hr), etoposide (100 μM; 24 hr) and STS (2 μM; 4 hr). Nontreated cells were transfected with nontargeting siRNA pool.

(D) ACHN cells transfected with the indicated siRNAs were treated with 200 ng/ml of anti-CD95 agonistic Ab (CH-11) for 6 hr. Relative caspase-3/7 activity (mean ± SD) was determined using the Caspase-Glo 3/7 assay. See also Figure S1 and Table S1.

apoptotic pathway. A search for interaction motifs within Atg12 identified a region bearing sequence similarity with BH3 domains (Figure 3A). Multiple sequence alignment revealed that this "BH3-like" region of Atg12 was conserved among several mammalian and nonmammalian vertebrate species (Figure S3A). Similar to proapoptotic BH3-only proteins of the Bcl-2 family, Atg12 did not contain other BH domains (BH1, BH2, or BH4). However, while BH3 domains assume a prototypical α-helical

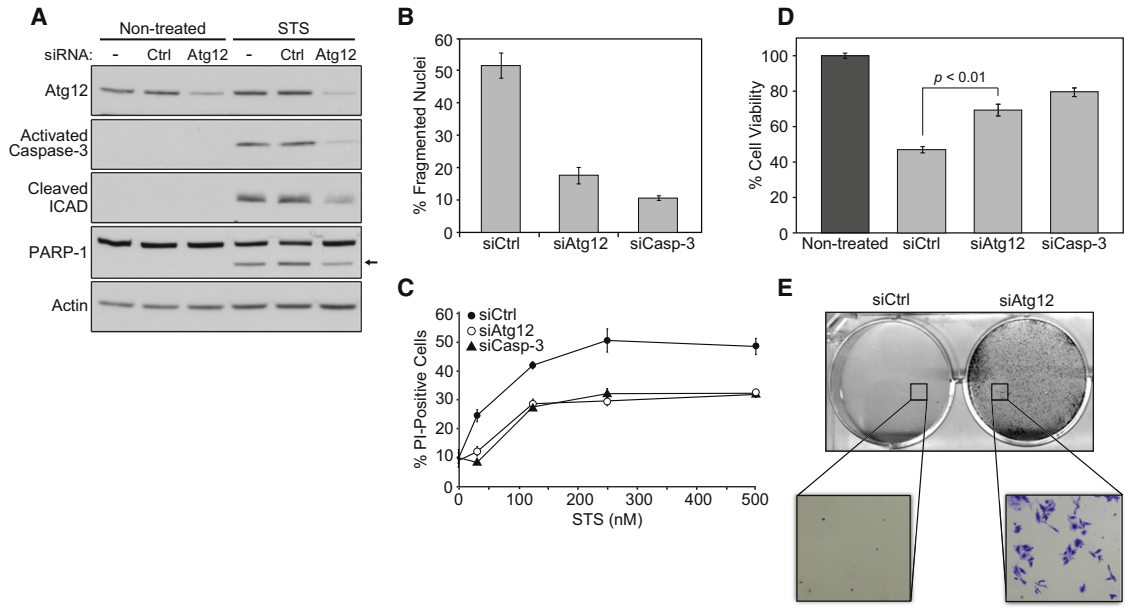

Figure 2. Depletion of Atg12 Increases Survival of Cells Undergoing Apoptotic Cell Death

(A) HeLa cells transfected with the indicated siRNAs were treated with STS (2 μM; 4 hr) and subjected to western blot analysis for molecular markers of apoptosis. Arrow indicates p85 cleaved form of PARP-1.

(B) STS-treated HeLa cells (0.5 μM; 8 hr) were fixed and stained with DAPI. Cells exhibiting nuclear fragmentation were counted under a fluorescence microscope. At least 200 cells were counted per sample in triplicates. Data represent mean ± SD of three independent measurements.

(C) HeLa cells transfected with the indicated siRNAs were treated with various concentrations of STS for 12 hr. The percent of PI-positive cells was determined by flow cytometry. Data represent mean ± SD of three replicate measurements.

(D) HeLa cells transfected with the indicated siRNAs were treated with 0.5 μM STS for 12 hr. Cell viability was assessed using the XTT colorimetric assay. Nontreated cells were transfected with nontargeting siRNA. Data represent mean ± SD of three replicate measurements.

(E) HeLa cells transfected with the indicated siRNAs were treated with 0.5 μM STS. After 12 hr, cells were trypsinized, replated, and incubated for 5 days in fresh medium. Surviving cells were fixed and stained with crystal violet dye. See also Figure S2.

fold, the BH3-like motif of Atg12 contains a conserved helix-breaking proline as one of the four residues that typically make up the hydrophobic face of BH3 helices (Figure 3A). Thus, despite sharing sequence similarity with BH3 domains, the BH3-like region of Atg12 is predicted to differ considerably in its structural fold.

The identification of a BH3-like region suggested that Atg12 may be able to interact with antiapoptotic Bcl-2 family members. Previous studies have demonstrated that while some BH3-only proteins are able to bind to all Bcl-2 antiapoptotic proteins, others exhibit selective binding to one of two protein subgroups, the first comprising Bcl-2, Bcl-X_L, and Bcl-w, and the second comprising Mcl-1 and A1 (Willis and Adams, 2005). We therefore proceeded to test whether Atg12 was able to interact with members of each subgroup, specifically Bcl-2 and Mcl-1. In transiently transfected HEK293 cells, wild-type Bcl-2 coimmunoprecipitated with FLAG-Atg12 (Figure 3B). In contrast, point mutation in the BH1 domain of Bcl-2 (Bcl-2 G145A) (Yin et al., 1994) completely abolished the interaction with Atg12, indicating that the binding requires the BH3-binding pocket of Bcl-2 (Figure 3B). The specificity of the interaction was further confirmed by reciprocal coimmunoprecipitation, in which FLAG-Bcl-2 pulled down ectopically expressed Atg12 (Figure S3B). In addition, Mcl-1 also coimmunoprecipitated with FLAG-Atg12 upon coexpression (Figure 3B), and FLAG-Atg12 interacted with endogenous Bcl-2 and Mcl-1 (Figure 3C). Thus, Atg12 is able to bind promiscuously to both subgroups of Bcl-2-related proteins. Finally, endogenous Atg12 coimmunoprecipitated with endogenous Mcl-1 in both HEK293 and HeLa cells, demonstrating that the interaction occurs in physiological conditions and in multiple cell types (Figure 3D). Interestingly, the binding of FLAG-Atg12 to endogenous Bcl-2 was increased in response to STS treatment in HeLa cells, without an apparent increase in protein levels (Figure 3E), implying that Atg12-Bcl-2 interaction may be regulated posttranslationally in response to apoptosis induction.

To further confirm that Atg12 binding occurs within the BH3-binding pocket of Bcl-2 family members, we examined the ability of known Bcl-2 inhibitors to compete out Atg12-Bcl-2 interaction. Indeed, the interaction between FLAG-Atg12 and endogenous Bcl-2 was disrupted by coexpression of the BH3-only protein Bad (Figure 3F) or by incubation of Atg12 immunoprecipitates with ABT-737, a small-molecule BH3 mimetic inhibitor of Bcl-2 (Figure 3G). Notably, the binding of Atg12 to Mcl-1 was not affected by ABT-737, which specifically targets Bcl-2 (Figure 3G).

In the yeast *Saccharomyces cerevisiae* and in *Drosophila melanogaster*, the BH3-like region of Atg12 deviates from the BH3 consensus motif; namely, a conserved Asp residue found in most BH3 domains (corresponding to D64 in hAtg12) is

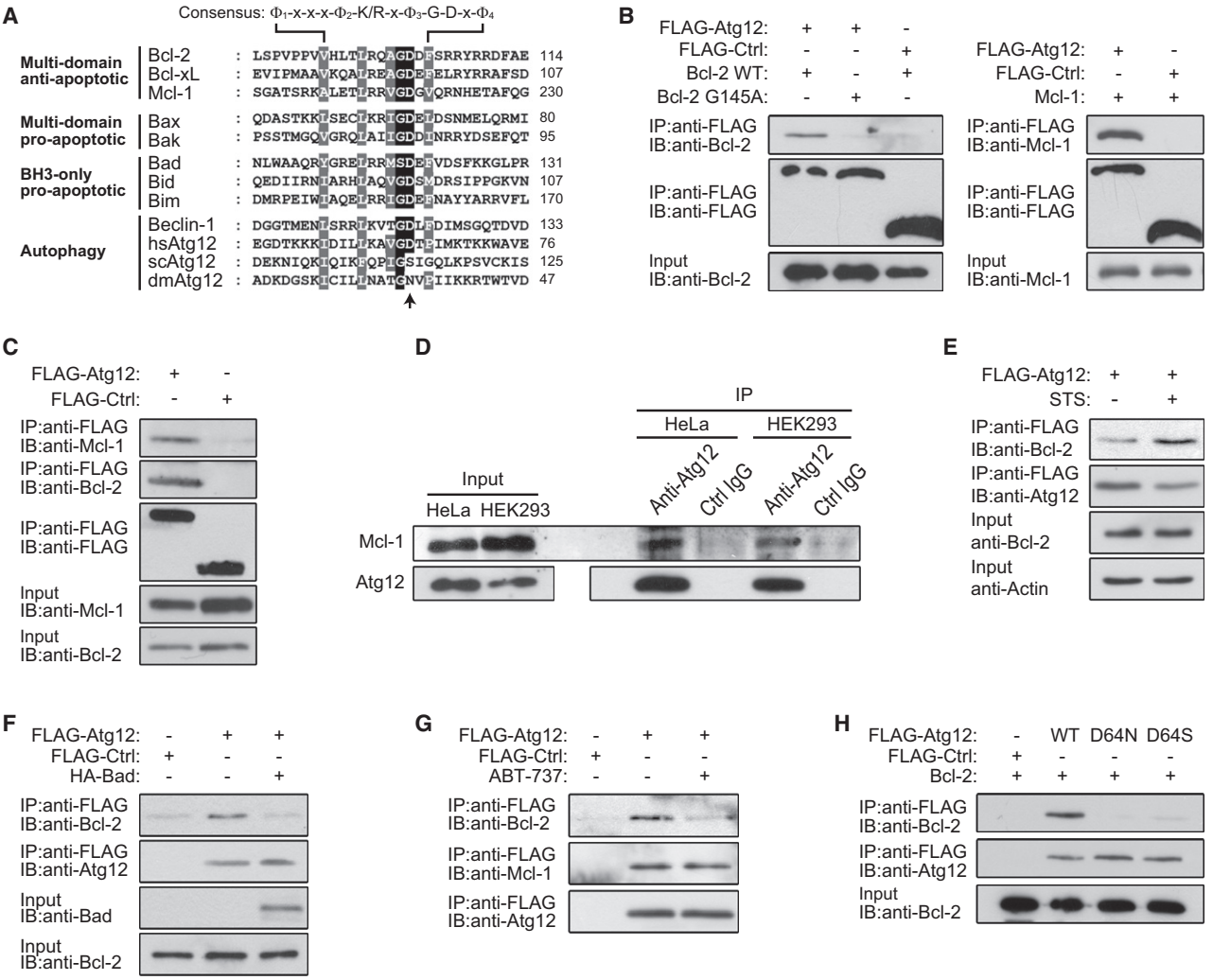

Figure 3. Atg12 Interacts with Bcl-2-Related Proteins via a BH3-like Motif

(A) Sequence alignment of the BH3-like region of Atg12 with BH3 domains of the Bcl-2 family using ClustalW. The four conserved BH3 hydrophobic residues are colored in gray, and the conserved "GD" residues in black. Arrow indicates critical Asp64 residue in hAtg12. Species abbreviations: Hs, *Homo sapiens*; Sc, *Saccharomyces cerevisiae;* Dm, *Drosophila melanogaster.*

(B) Coimmunoprecipitation of FLAG-tagged hAtg12 and Bcl-2 or Mcl-1 from HEK293 cells cotransfected as indicated.

(C) Coimmunoprecipitation of FLAG-tagged hAtg12 with endogenous Bcl-2 and Mcl-1 from HEK293 cells.

(D) Coimmunoprecipitation of endogenous Atg12 and endogenous Mcl-1 in HEK293 and HeLa cells. Mouse anti-Cytokeratin18 was used as control IgG.

(E) Coimmunoprecipitation of FLAG-tagged Atg12 and endogenous Bcl-2 in HeLa cells treated with STS (3 μM; 4 hr).

(F) Coimmunoprecipitation of FLAG-tagged Atg12 and endogenous Bcl-2 in HEK293 cells coexpressing a control plasmid (CAT) or HA-tagged BAD.

(G) FLAG-Atg12 was immunoprecipitated from HEK293 cells and incubated with either 10 μM ABT-737 or DMSO (vehicle control). Coprecipitating Bcl-2 was assessed by western blot after elution with excess FLAG peptide.

(H) Coimmunoprecipitation of wild-type Atg12 or Atg12/D64 mutants with Bcl-2 in HEK293 cells cotransfected as indicated. In (B), (C), and (F)–(H), DAP1-FLAG was used as a negative control for coimmunoprecipitation. See also Figure S3.

replaced by Ser in yeast and Asn in flies (Figure 3A, denoted by arrow). Notably, this Asp is known to be critical for the binding of BH3-only proteins to antiapoptotic Bcl-2 members. The sequence variability observed in scAtg12 and dmAtg12 suggested that functionality of the BH3-like region of Atg12 might not extend to these organisms. Indeed, binding of Atg12 to Bcl-2 was severely impaired upon mutation of the conserved D64 in the BH3-like region of hAtg12 to Ser or Asn, resembling the sequences of scAtg12 and dmAtg12, respectively (Figure 3H). No effect on binding was observed when D64 was substituted to Ala (data not shown). This is particularly interesting, as the fly lacks canonical counterparts of BH3-only proteins, and yeast lack homologs of the antiapoptotic Bcl-2 proteins.

Taken together, the data suggest that Atg12 binds to several Bcl-2 family members, and that both the BH3-like region of Atg12 and the BH3-binding groove of Bcl-2 are necessary for the interaction. Notably, although capable of interacting with both subgroups of antiapoptotic Bcl-2 members, Atg12 did not

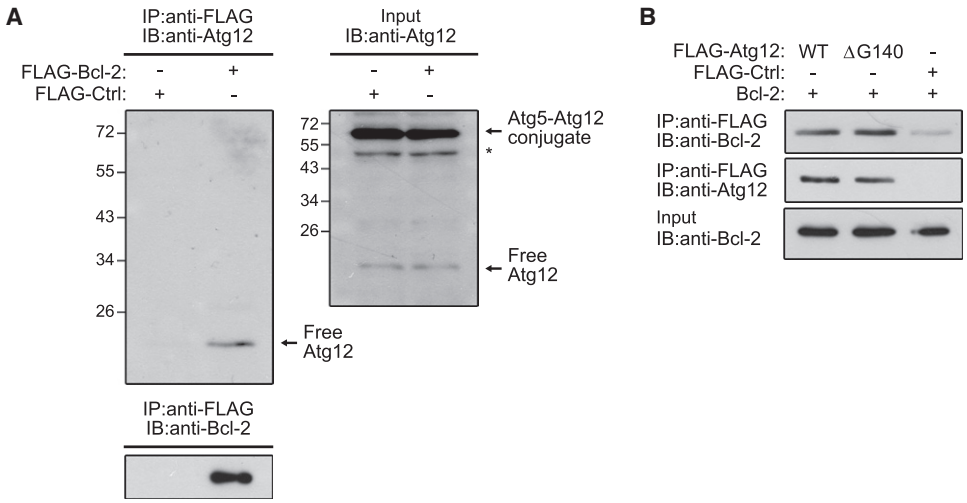

Figure 4. Atg12 Binding to Bcl-2 Does Not Require Conjugation Activity

(A) Coimmunoprecipitation of endogenous Atg12 in HEK293 cells expressing FLAG-tagged Bcl-2. DAP1-FLAG was used as a negative control. Asterisk indicates nonspecific band.

(B) Coimmunoprecipitation of wild-type Atg12 or a conjugation-defective (ΔG140) mutant with Bcl-2 in transiently transfected HEK293 cells. DAP1-FLAG was used as a negative control. See also Figure S4.

associate with endogenous or ectopically expressed Bax, a multidomain proapoptotic protein of the Bcl-2 family (data not shown). Thus, in contrast to certain BH3-only proteins, such as tBid, Atg12 is unlikely to induce Bax activation directly.

Atg12 Interaction with Bcl-2 Does Not Require Conjugation Activity

The conjugation of Atg12 to Atg5 is an essential step in the process of autophagy. In order to establish whether Bcl-2 binds to free Atg12, or to the Atg5-Atg12 conjugate, the nature of endogenous Atg12 that is coimmunoprecipitated with Bcl-2 was examined more closely. Upon immunoprecipitation of FLAG-tagged Bcl-2 from HEK293 cells, a single band corresponding to the size of unconjugated Atg12 was observed, with no traces at the expected conjugate size (Figure 4A, left). Furthermore, neither of Atg12's reported conjugation partners, Atg5 or Atg3, could be detected on this blot (data not shown). Likewise, overexpressed Atg5 did not coimmunoprecipitate with Bcl-2 in transiently transfected HEK293 cells, in agreement with previous observations (Figure S4A; Yousefi et al., 2006). The interaction between Bcl-2 and free Atg12 is significant, considering that unconjugated Atg12 represents only a small fraction of cellular Atg12, whereas the majority of the protein is conjugated to Atg5, even under basal conditions when autophagy is not induced (Figure 4A, right).

To further confirm that unconjugated Atg12 is sufficient for interaction with Bcl-2, cells were transfected with a mutant Atg12 lacking the C-terminal Gly that is essential for conjugation with Atg5 or Atg3 (Atg12ΔG140). The conjugation-defective mutant was able to bind Bcl-2 with the same efficiency as WT Atg12 (Figure 4B), indicating that the interaction with Bcl-2 family members is mediated exclusively by Atg12 and does not require the ubiquitin-like conjugation machinery.

Recently, disruption of Atg12 conjugation to Atg3 by knockout of Atg3 in mouse embryonic fibroblasts (MEFs) was shown to upregulate levels of Bcl-X_L, leading to inhibition of mitochondria-based apoptosis (Radoshevich et al., 2010). In our experimental system, however, expression levels of Bcl-X_L and other antiapoptotic members of the Bcl-2 family remained unchanged in response to disruption of Atg12-Atg3 conjugation by knockdown of either Atg12 (Figure S4B) or Atg3 (Figure S4C). Moreover, and in strong contrast to Atg12, the knockdown of Atg3 with five different siRNAs did not reduce caspase activity in etoposide-treated HEK293 cells (Figure S4D) or STS-treated HeLa cells (data not shown). Thus, the outcome of Atg12 depletion on apoptosis reported here cannot be attributed to its conjugation to Atg3.

Structural Insights into the Mechanism of Atg12-Mcl-1 Interaction by Computational Docking

The presence of a helix-breaking proline within the BH3-like motif of Atg12 suggested that Atg12 may differ considerably from BH3-only proteins in its mode of interaction with Bcl-2 family members. To gain insight on this matter, in silico protein-protein docking was used to model the interaction with Bcl-2 family proteins. The structure of hAtg12 was modeled based on plant Atg12 (Suzuki et al., 2005), available from the Protein Data Bank (PDB) (Berman et al., 2000). The sequences of plant and human Atg12 exhibit 42% identity along the whole polypeptide chain, rendering the plant structure an adequate modeling template. The crystal structure of plant Atg12 is of a homodimer with domain swapping, and the loop 105-NQSF-108 of the Atg12 monomer was modeled to connect the swapped domains. As predicted from the protein sequence, the BH3-like motif of Atg12 did not form an α-helix, but rather a loop comprising residues 62-VGDTPIK-68, of which D64 is involved in the binding of Bcl-2. The structure of loop 93-KLVAS-97, which is three residues longer in the modeled sequence, was determined using molecular dynamics. Notably, this loop is spatially adjacent to the BH3-like region.

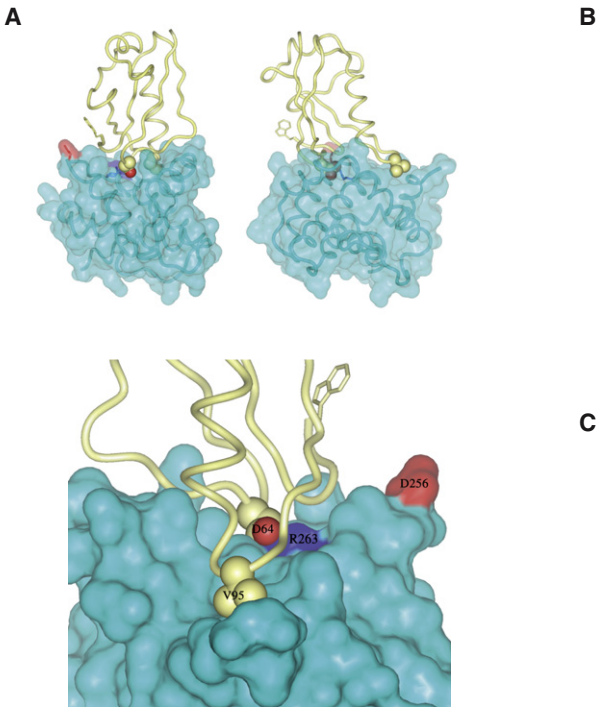

Figure 5. In Silico Model of Atg12-Mcl-1 Interaction

(A) The predicted mode of interaction between Atg12 and Mcl-1 based on protein-protein docking. Atg12 is depicted by a yellow ribbon diagram. Only the side chains of residues D64 and V95 are shown as space-filling spheres, colored by atom type (yellow for C and red for O). Mcl-1 is shown in cyan with R263 emphasized in blue and D256 in red. Top panel: two views from 90° rotation about the vertical axis. Bottom panel: a close-up view of the hydrophobic cleft region of Mcl-1.

(B) Coimmunoprecipitation of WT Atg12 or Atg12/V95A mutant with Mcl-1 in transiently transfected HEK293 cells.

(C) Coimmunoprecipitation of Atg12 with WT Mcl-1 or Mcl-1/R263A mutant in transiently transfected HEK293 cells. See also Figure S5.

As both Bcl-2 and Mcl-1 change conformation upon ligand binding, we expected that the conformer that binds Atg12 would be more similar to the ligand-bound protein than to the free protein. Therefore, the final model of Atg12 was docked to Mcl-1, since a high-resolution structure of this protein with a bound ligand was available.

Docking models were generated using a comprehensive geometric-electrostatic-hydrophobic (GEH) scan performed with the program MolFit (Berchanski et al., 2004), followed by a postscan filter that tests statistical propensity measures and estimates the desolvation energy of the predicted interfaces (Kowalsman and Eisenstein, 2009). Six hundred ten models passed this filter. At this point, biological information was introduced, and only models that involved the BH3-binding cavity of Mcl-1 and residue D64 of Atg12 at the interface were retained, producing 14 possible models. The energy-minimized top-ranking model is shown in Figure 5A. According to the model, the intramolecular ion pair of Mcl-1 R263/D256 is predicted to be broken upon Atg12 binding and replaced by an intermolecular ion pair with Atg12/D64. The docking model also predicted that additional hydrophobic contacts with the BH3-binding cavity are made by Atg12/V95 from the adjacent loop 93-97.

The hypothetical model was then experimentally tested by mutating the residues in Atg12 and Mcl-1 that were predicted to form crucial contact points. Coimmunoprecipitation experiments indicated that mutation of Atg12/V95 to Ala severely reduced the ability of Atg12 to interact with Mcl-1 (Figure 5B). Additionally, mutation of Mcl-1/R263, which was predicted to interact with Atg12/D64 from the BH3-like region, resulted in decreased coimmunoprecipitation with FLAG-Atg12 (Figure 5C). In contrast, mutation of residues in Atg12 that were not predicted to contribute to the interaction with Mcl-1, e.g., substitution of F101 (Figure S5) and T65 (data not shown) to Ala, did not affect levels of coimmunoprecipitated Mcl-1. Thus, the computational model accurately predicted critical contact points between Atg12 and Mcl-1, providing the means to generate mutants for further experimental assessment of the functional significance of this interaction.

Atg12 Functions Upstream of Mitochondrial Outer Membrane Permeabilization (MOMP)

To determine whether Atg12 promotes apoptosis in a similar manner to BH3-only proteins, by antagonizing the function of prosurvival Bcl-2 members, we assessed the functional implications of the Atg12-Mcl-1 interaction. To this end, HeLa cells were transfected with increasing amounts of Mcl-1 plasmid, alone or in combination with Atg12. Expression of Mcl-1 together with a control plasmid (CAT) protected HeLa cells from STS-induced apoptosis in a dose-dependent manner (Figure 6A). Coexpression of Atg12, however, mitigated the protective effect of Mcl-1, leading to increased caspase activity. Strikingly, the ability of Atg12 to antagonize Mcl-1 was completely abolished when the Mcl-1 binding-defective mutant of Atg12 (V95A) was expressed, suggesting that the proapoptotic function of Atg12 is dependent on its ability to bind prosurvival Bcl-2 members. In contrast, the conjugation-defective mutant (ΔG140) behaved similarly to WT Atg12, indicating that conjugation to Atg5 or Atg3 is not required for suppression of Mcl-1 by Atg12 (Figure 6B). Notably, overexpression of Atg12 alone was not sufficient to induce apoptosis (data not shown).

Next, we assessed whether the depletion of Atg12 affected early events in the apoptotic cascade that are regulated by anti-apoptotic Bcl-2 proteins. In HeLa cells, treatment with STS led to activation of Bax, as determined by a conformation-specific antibody (6A7) that recognizes activated Bax. In contrast, Bax activation was almost completely blocked in response to Atg12 depletion (Figure 6C). Importantly, Bax activation was restored upon enforced expression of an siRNA-resistant

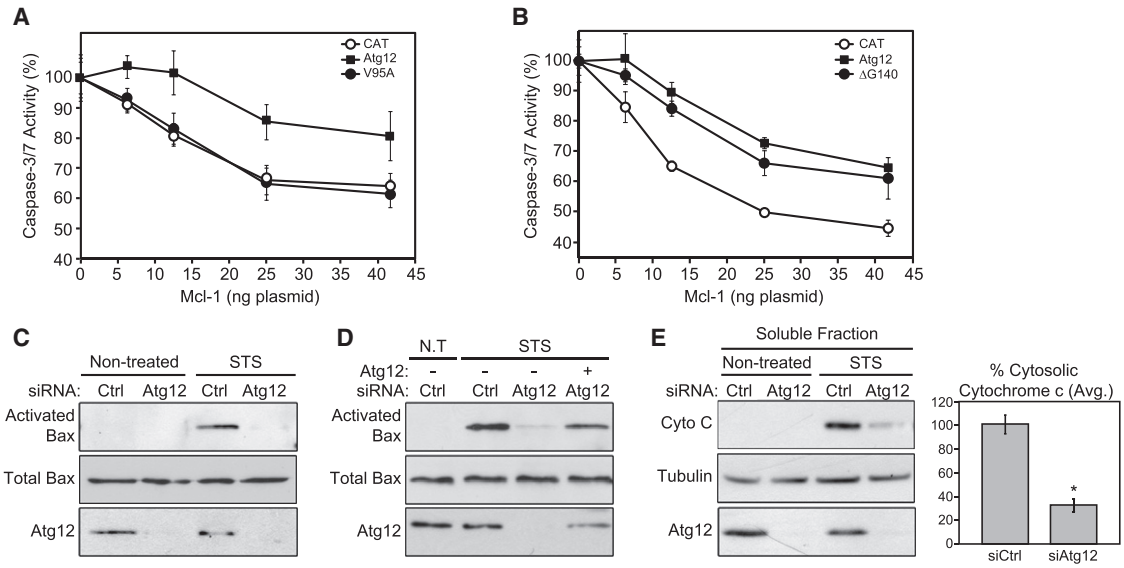

Figure 6. Atg12 Functions Upstream of MOMP

(A and B) Relative caspase-3/7 activity in STS-treated HeLa cells (2 μM; 4 hr) transfected with increasing amounts of Mcl-1 plasmid together with: (A) CAT (control), WT Atg12, or Atg12/V95A mutant; or with: (B) CAT (control), WT Atg12, or ΔG140 mutant. Results represent mean ± SD of combined data from three independent experiments.

(C) Immunoprecipitation of conformationally active Bax from STS-treated HeLa cells transfected with the indicated siRNAs.

(D) HeLa cells were cotransfected with the indicated siRNAs together with plasmids encoding for either CAT (control) or siRNA-resistant Atg12. Active Bax was immunoprecipitated 48 hr posttransfection, following treatment with STS (2 μM; 4 hr). N.T., nontreated.

(E) HeLa cells transfected with the indicated siRNAs were treated with STS (2 μM; 4 hr), and subjected to subcellular fractionation by differential centrifugation. Left panel: representative fractionation experiment. Tubulin was used as a cytosolic (soluble fraction) marker. Purity of cytosolic fractions was verified by blotting with a mitochondrial marker (Grp-75). Right panel: quantitation of cytosolic cytochrome c levels following siRNA-mediated depletion of Atg12 relative to nontargeting control by densitometric analysis. Results represent mean ± SD of combined data from three independent fractionation experiments. Asterisk denotes $p < 0.05$.

construct of Atg12 (Figure 6D). Consistent with reduced Bax activation, release of cytochrome c from mitochondria to the cytosol, a key step in the initiation of apoptosis, was also significantly attenuated in Atg12-depleted cells (Figure 6E). Hence, the apoptotic function of Atg12 lies upstream of mitochondrial outer membrane permeabilization (MOMP), consistent with inhibition of antiapoptotic Bcl-2-related proteins.

Bcl-2 Binding-Deficient Mutants of Atg12 Retain Autophagic Function

Next, we assessed whether the mutations in the BH3-like region that abolished the interaction with Bcl-2 also affected the canonical function of Atg12 in autophagy. To this end, reconstitution assays were performed in HEK293 cells stably expressing GFP-LC3, in which endogenous Atg12 was knocked down by siRNA. In Atg12-depleted cells, ectopic expression of siRNA-resistant constructs of WT Atg12 or the BH3 D64S/N mutants restored levels of the Atg5-Atg12 conjugate (Figure 7B), indicating that the conjugation process was not impaired by mutations in the BH3-like region. Autophagy levels were then measured by following the distribution pattern of GFP-LC3. In response to induction of autophagy by nutrient deprivation, GFP-LC3 redistributes from diffuse cytoplasmic localization to punctate structures that correspond to autophagosomal membranes and is thus widely used as a marker for autophagic activity. As expected, in Atg12-depleted cells undergoing starvation, GFP-LC3 was mostly diffuse throughout the cytoplasm, reflecting a defect in autophagosome formation (Figure 7A). In contrast, GFP-LC3 displayed clear punctate staining when Atg12-depleted cells were reconstituted with either WT Atg12 or the Bcl-2 binding-deficient mutants (Figure 7A), indicating that autophagy was restored. This was also reflected by examining the ratio between the two LC3 forms by western blot analysis (Figure S6). Similarly, while p62, a specific target of autophagy that is used as a marker for autophagic flux, accumulated in Atg12-depleted cells undergoing starvation, its levels were significantly reduced upon reintroduction of either WT Atg12 or the BH3-like mutants (Figures 7B and S6). Taken together, the data suggest that the Bcl-2 binding-deficient mutants of Atg12 retain autophagic function. Thus, the apoptotic and autophagic functions of Atg12 seem to be independent arms of the protein.

DISCUSSION

Our results suggest that in addition to its canonical role in autophagy, the ubiquitin-like protein Atg12 functions as a positive mediator of mitochondrial apoptosis through inhibitory interactions with antiapoptotic Bcl-2 family members upstream of MOMP. Atg12 was required for the induction of apoptosis in multiple cell types and triggers, suggesting that its proapoptotic function is of physiological relevance.

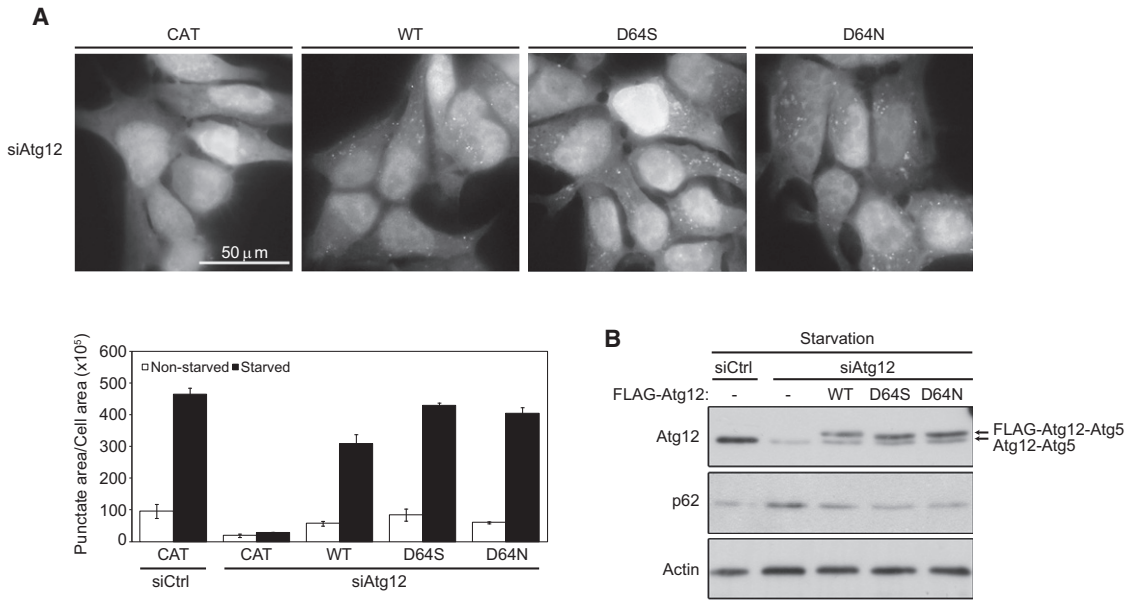

Figure 7. Bcl-2 Binding-Defective Mutants of Atg12 Retain Autophagic Activity

(A) Top panel: representative images of GFP-LC3 staining in Atg12-depleted HEK293 cells undergoing starvation (EBSS; 4 hr). Cells were reconstituted with siRNA-resistant constructs expressing FLAG-tagged WT Atg12 or the Bcl-2 binding-defective mutants (D64N/S). Bottom panel: quantitation of GFP-LC3 puncta per total cell area. Data represent mean ± SD of triplicate measurements of at least 200 cells each.

(B) Western blot analysis displaying reconstitution of the Atg5-Atg12 conjugate in cell lysates taken from GFP-LC3 HEK293 cells analyzed in (A). Specific autophagic degradation of p62 serves as indication of autophagic flux. See also Figure S6.

We found that Atg12 contains a region with sequence similarity to BH3-domains that is required for its interaction with Bcl-2. Homology modeling combined with computational protein-protein docking analysis revealed that unlike BH3-only proteins, which are characterized by a canonical α-helical BH3 domain, the BH3-like motif of Atg12 is predicted to form a loop that binds to the hydrophobic cleft of Bcl-2 family members together with a second adjacent loop. The fundamental differences between canonical BH3 domains and the BH3-like region of Atg12 suggest that Atg12 cannot be classified as a member of the BH3-only family, and may represent a unique mode of interaction with antiapoptotic Bcl-2 proteins. Yet, despite these structural differences, our data indicate that Atg12 shares several functional similarities with proteins belonging to this family: Atg12 was able to interact with multiple prosurvival Bcl-2 family members, as demonstrated for Bcl-2 and Mcl-1; the interaction required both the BH3-like region of Atg12 and the BH3-binding groove of Bcl-2 and Mcl-1; binding of Atg12 to Mcl-1 suppressed its antiapoptotic activity; and Atg12 was necessary for Bax activation upstream of MOMP. The significance of the structural differences is not known, but may enable specific regulation of the Atg12-Bcl-2 interaction.

Coimmunoprecipitation studies indicated that Bcl-2 interacted exclusively with free, unconjugated Atg12, which does not have a role in autophagy. Consistent with this finding, an autophagy-deficient mutant of Atg12 incapable of undergoing conjugation to Atg5 (or Atg3) was equivalent to WT Atg12 in its ability to interact with Bcl-2 and to suppress the antiapoptotic function of Mcl-1. In contrast, disruption of the interaction with Bcl-2 proteins abrogated the apoptotic function of Atg12, but did not impair its autophagic function. Taken together, the data suggest that Atg12's apoptotic function, via noncovalent binding to Bcl-2 family members, and autophagic function, via covalent conjugation to Atg5, are distinct properties of the protein. In addition, activities related to the Atg3-Atg12 conjugate, such as regulation of Bcl-X_L levels (Radoshevich et al., 2010), were not observed here. Accordingly, knockdown of Atg3 did not reproduce the effects of Atg12 knockdown on caspase activation in our system, indicating that the molecular mechanism that underlies the apoptotic function of Atg12 reported here clearly represents a distinct mechanism. In this regard, the role of Atg12 shown here as a regulator of caspase-dependent cell death also differs from that described previously, in which Atg12 was shown to preserve cell viability when apoptosis was triggered in the presence of caspase inhibitors, probably as part of its autophagic role (Colell et al., 2007).

In evolutionary terms, autophagy is likely a more ancient process than apoptosis (Schwartz et al., 1993). In yeast, autophagy is carried out in a manner similar to higher eukaryotes and, in fact, most of the known mammalian autophagy genes were identified based on their homology to yeast (Nakatogawa et al., 2009). In contrast, part of the molecular machinery involved in the regulation and execution of mammalian apoptosis, including the antiapoptotic Bcl-2 proteins, is absent in yeast. Similarly, although counterparts of the core apoptotic proteins have been identified in *Drosophila*, it lacks orthologs of canonical BH3-only proteins. Indeed, we found that the BH3-like regions of yeast and fly Atg12 possess a single amino acid substitution that, when introduced into the human Atg12 sequence, renders the protein unable to interact with Bcl-2. Hence, it appears that

the apoptotic BH3-like function of Atg12 may be unique to higher organisms. It is tempting to speculate that the ability of Atg12 to associate with Bcl-2 proteins evolved concomitantly with apoptosis to accommodate a direct molecular crosstalk between the two processes.

In fact, crosstalk between the apoptotic and autophagic machineries is emerging as a recurring theme, with particular importance for Bcl-2 family proteins in bridging the two pathways. A recent paper reported that UVRAG, a regulator of autophagy that interacts with the Vps34 PI3K/Beclin-1 complex, inhibits apoptosis by direct association with Bax, which blocks its activation and translocation to mitochondria (Yin et al., 2011). Thus, UVRAG and Atg12 mediate opposing effects on mitochondria-based apoptotic signaling. Although in both cases the autophagic function of the protein was not necessary for its function in apoptosis, the dual nature of these proteins suggests that crosstalk between the two pathways is important both to activate and inhibit apoptosis. Further study is required in order to fully elucidate the physiological implications of these interactions. For example, it is possible that under specific stress conditions autophagy is initially induced in an attempt to mitigate the insult and sustain viability, while apoptosis is actively suppressed by UVRAG, but if the stress persists, binding of Atg12 to Bcl-2 may then function as a molecular switch to facilitate the activation of apoptosis.

In the opposite direction, antiapoptotic Bcl-2 members, including Bcl-2 and Mcl-1, suppress autophagy by binding to the essential autophagy protein Beclin-1 (Germain et al., 2011; Pattingre et al., 2005). The interaction between Bcl-2 proteins and Beclin-1 requires the BH3 domain of the latter (Sinha and Levine, 2008) and can be inhibited by proapoptotic BH3-only proteins (Maiuri et al., 2007a). For reasons that remain unclear, the outcome of Bcl-2 binding to Beclin-1 appears to be unidirectional and results in inhibition of autophagy without a reciprocal effect on apoptosis (Boya and Kroemer, 2009; Ciechomska et al., 2009), in contrast to Atg12's ability to antagonize the antiapoptotic activity of Mcl-1. Hence, although Beclin-1 and Atg12 are both able to bind Bcl-2 family members, they differ considerably in their mechanism of binding and the functional outcome of the interaction. A possible explanation for this dichotomy may reside in differential binding affinities of the proteins to Bcl-2.

Prosurvival Bcl-2 proteins are overexpressed in many types of tumors, rendering cells refractory to chemotherapeutic agents that induce apoptosis. Targeting Bcl-2-related proteins with BH3 mimetic compounds is therefore a promising emerging strategy for therapy in these types of tumors (Leber et al., 2010). Our finding that Atg12 binds to both subgroups of antiapoptotic Bcl-2 proteins, together with the prediction that the mechanism of binding differs from that of classical BH3-only proteins, point to Atg12 as a possible candidate for future study of its potential as a basis for drug design.

EXPERIMENTAL PROCEDURES

siRNA Screening and Caspase Activity Assay

HEK293 cells were reverse-transfected in 96-well plates with 50 nM of the indicated siGENOME siRNA pools (Dharmacon) using DharmaFECT4 transfection reagent (Dharmacon). Cells were treated 24 hr posttransfection with 50 μM etoposide (Sigma-Aldrich) for a period of 48 hr. Caspase activity was measured using the Caspase-Glo 3/7 luminescent assay (Promega), according to the manufacturer's instructions. Plates were read using the Veritas microplate luminometer (Turner BioSystems). siRNA targeting caspase-3 was used as a positive control, while nontargeting pool, RISC-free siRNA, and mock transfection were used as negative controls. The average caspase activity of negative controls was defined as 100% caspase activity. A similar protocol was used for hit validation using ON-TARGET*plus* siRNA pools (Dharmacon) and individual siRNA duplexes (Sigma-Aldrich). In the latter experiment, Sigma universal siRNA control #1 was used as an additional negative control. For cell number determination, DNA content was measured in parallel plates using the CyQUANT NF cell proliferation assay (Invitrogen).

Data from three biological repeats of the primary screen were normalized in an experiment-wise manner according to the sample median of each screen. All siRNAs were screened in three replicate wells per plate. Positive hits were defined as genes whose knockdown led to a statistically significant ($p < 0.01$) decrease in caspase activity compared to the group of nontargeting controls in a Student's two-tailed t test in all three biological repeats of the screen.

Cell Viability

Cell viability was assessed using the XTT colorimetric assay according to the manufacturer's instructions (Biological Industries). Absorbance was read in a microplate ELISA reader (Bio-Tek) at 450 nm. Membrane integrity was evaluated by propidium iodide (PI) uptake; PI (25 μg/ml; Sigma-Aldrich) was added to cells immediately prior to analysis by flow cytometry (FACScan; Beckton Dickinson).

Clonogenic Survival

siRNA-transfected HeLa cells were treated with 0.5 μM STS for 15 hr, washed, and replated onto 6-well plates. Cells were allowed to grow for 5 days, fixed in 3.7% formaldehyde, and stained with 0.05% (w/v) crystal violet (Sigma-Aldrich). Surviving cells were imaged using a binocular microscope (Leica MZ16F).

Immunoprecipitation

For coimmunoprecipitation, HEK293 cells were transiently transfected with the indicated plasmids. Cell pellets were lysed in B buffer (0.4% NP-40, 0.5 mM EDTA, 100 mM KCl, 20 mM HEPES [pH 7.6], 20% glycerol) supplemented with protease and phosphatase inhibitors. Following preclearance with protein G PLUS-Agarose beads (Santa Cruz Biotechnology), extracts were incubated with anti-FLAG M2 beads (Sigma-Aldrich) for 2 hr, eluted with excess FLAG peptide (Sigma-Aldrich), and subjected to western blot analysis. An irrelevant tagged protein was used as a negative control where indicated.

For endogenous IPs, mouse monoclonal antibody against Atg12 (MBL) was used for immunoprecipitation of Atg12. Detection of Mcl-1 was carried out with mouse anti-Mcl-1 (RC13, Santa Cruz Biotechnology) followed by incubation with rat anti-mouse Ig, kappa light chain secondary antibody (BD PharMingen) to avoid detection of Ab heavy chain. Mouse anti-Cytokeratin18 (Santa Cruz Biotechnology) was used as a negative control.

Conformationally active Bax was immunoprecipitated with anti-Bax antibody (6A7, Abcam). Cell pellets from STS-treated HeLa cells (3 μM, 4 hr; Sigma-Aldrich) were resuspended in 1% CHAPS (3-[(3-cholamidopropyl)-dimethylammonio]-1-propanesulfonate) buffer supplemented with protease and phosphatase inhibitors. Precleared cell lysates were incubated with 2 μg antibody overnight at 4°C, followed by incubation with protein G agarose beads. Beads were washed with lysis buffer and boiled in sample buffer. Western blot detection of total Bax was performed with anti-Bax N20 antibody (Santa Cruz Biotechnology).

GFP-LC3 Punctate Staining

HEK293 cells stably expressing GFP-LC3 were plated onto 13 mm glass coverslips coated with poly-L-Lysine (Sigma-Aldrich), and subjected to starvation for 4 hr in Earl's Balanced Salt Solution (EBSS; Biological industries). Cells were fixed in 3.7% formaldehyde and viewed by fluorescence microscopy (Olympus BX41) with 60× (N.A. 1.25) UPlan-FI oil immersion objectives. Digital images were obtained with a DP50 CCD camera using ViewfinderLite and StudioLite software (Olympus). The percentage of puncta area per total

cell area was determined using MetaMorph imaging software (Molecular Devices).

SUPPLEMENTAL INFORMATION

Supplemental Information includes six figures, one table, Supplemental Experimental Procedures, and Supplemental References and can be found with this article online at doi:10.1016/j.molcel.2011.10.014.

ACKNOWLEDGMENTS

We thank E. Feldmesser from the Bioinformatics and Biological Computing Unit at the Weizmann Institute of Science and P. Kohonen from VTT Medical Biotechnology, Finland, for their assistance with statistical analysis. This work was supported by a Center of Excellence grant from the Flight Attendant Medical Research Institute (FAMRI). A.K. is the incumbent of the Helena Rubinstein Chair of Cancer Research.

Received: March 17, 2011
Revised: September 7, 2011
Accepted: October 10, 2011
Published: December 8, 2011

REFERENCES

Barnhart, B.C., Legembre, P., Pietras, E., Bubici, C., Franzoso, G., and Peter, M.E. (2004). CD95 ligand induces motility and invasiveness of apoptosis-resistant tumor cells. EMBO J. *23*, 3175–3185.

Berchanski, A., Shapira, B., and Eisenstein, M. (2004). Hydrophobic complementarity in protein-protein docking. Proteins *56*, 130–142.

Berman, H.M., Westbrook, J., Feng, Z., Gilliland, G., Bhat, T.N., Weissig, H., Shindyalov, I.N., and Bourne, P.E. (2000). The Protein Data Bank. Nucleic Acids Res. *28*, 235–242.

Berry, D.L., and Baehrecke, E.H. (2007). Growth arrest and autophagy are required for salivary gland cell degradation in Drosophila. Cell *131*, 1137–1148.

Boya, P., and Kroemer, G. (2009). Beclin 1: a BH3-only protein that fails to induce apoptosis. Oncogene *28*, 2125–2127.

Cho, D.H., Jo, Y.K., Hwang, J.J., Lee, Y.M., Roh, S.A., and Kim, J.C. (2009). Caspase-mediated cleavage of ATG6/Beclin-1 links apoptosis to autophagy in HeLa cells. Cancer Lett. *274*, 95–100.

Ciechomska, I.A., Goemans, G.C., Skepper, J.N., and Tolkovsky, A.M. (2009). Bcl-2 complexed with Beclin-1 maintains full anti-apoptotic function. Oncogene *28*, 2128–2141.

Colell, A., Ricci, J.E., Tait, S., Milasta, S., Maurer, U., Bouchier-Hayes, L., Fitzgerald, P., Guio-Carrion, A., Waterhouse, N.J., Li, C.W., et al. (2007). GAPDH and autophagy preserve survival after apoptotic cytochrome c release in the absence of caspase activation. Cell *129*, 983–997.

Denton, D., Shravage, B., Simin, R., Mills, K., Berry, D.L., Baehrecke, E.H., and Kumar, S. (2009). Autophagy, not apoptosis, is essential for midgut cell death in Drosophila. Curr. Biol. *19*, 1741–1746.

Eisenberg-Lerner, A., Bialik, S., Simon, H.U., and Kimchi, A. (2009). Life and death partners: apoptosis, autophagy and the cross-talk between them. Cell Death Differ. *16*, 966–975.

Erlich, S., Mizrachy, L., Segev, O., Lindenboim, L., Zmira, O., Adi-Harel, S., Hirsch, J.A., Stein, R., and Pinkas-Kramarski, R. (2007). Differential interactions between Beclin 1 and Bcl-2 family members. Autophagy *3*, 561–568.

Germain, M., Nguyen, A.P., Le Grand, J.N., Arbour, N., Vanderluit, J.L., Park, D.S., Opferman, J.T., and Slack, R.S. (2011). MCL-1 is a stress sensor that regulates autophagy in a developmentally regulated manner. EMBO J. *30*, 395–407. Published online December 7, 2010. 10.1038/emboj.2010.327.

Gozuacik, D., Bialik, S., Raveh, T., Mitou, G., Shohat, G., Sabanay, H., Mizushima, N., Yoshimori, T., and Kimchi, A. (2008). DAP-kinase is a mediator of endoplasmic reticulum stress-induced caspase activation and autophagic cell death. Cell Death Differ. *15*, 1875–1886.

Jackson, A.L., Burchard, J., Leake, D., Reynolds, A., Schelter, J., Guo, J., Johnson, J.M., Lim, L., Karpilow, J., Nichols, K., et al. (2006). Position-specific chemical modification of siRNAs reduces "off-target" transcript silencing. RNA *12*, 1197–1205.

Kowalsman, N., and Eisenstein, M. (2009). Combining interface core and whole interface descriptors in postscan processing of protein-protein docking models. Proteins *77*, 297–318.

Kuma, A., Mizushima, N., Ishihara, N., and Ohsumi, Y. (2002). Formation of the approximately 350-kDa Apg12-Apg5.Apg16 multimeric complex, mediated by Apg16 oligomerization, is essential for autophagy in yeast. J. Biol. Chem. *277*, 18619–18625.

Leber, B., Geng, F., Kale, J., and Andrews, D.W. (2010). Drugs targeting Bcl-2 family members as an emerging strategy in cancer. Expert Rev. Mol. Med. *12*, e28.

Levine, B., and Kroemer, G. (2008). Autophagy in the pathogenesis of disease. Cell *132*, 27–42.

Luo, S., and Rubinsztein, D.C. (2010). Apoptosis blocks Beclin 1-dependent autophagosome synthesis: an effect rescued by Bcl-xL. Cell Death Differ. *17*, 268–277.

Maiuri, M.C., Criollo, A., Tasdemir, E., Vicencio, J.M., Tajeddine, N., Hickman, J.A., Geneste, O., and Kroemer, G. (2007a). BH3-only proteins and BH3 mimetics induce autophagy by competitively disrupting the interaction between Beclin 1 and Bcl-2/Bcl-X(L). Autophagy *3*, 374–376.

Maiuri, M.C., Zalckvar, E., Kimchi, A., and Kroemer, G. (2007b). Self-eating and self-killing: crosstalk between autophagy and apoptosis. Nat. Rev. Mol. Cell Biol. *8*, 741–752.

Nakatogawa, H., Suzuki, K., Kamada, Y., and Ohsumi, Y. (2009). Dynamics and diversity in autophagy mechanisms: lessons from yeast. Nat. Rev. Mol. Cell Biol. *10*, 458–467.

Pattingre, S., Tassa, A., Qu, X., Garuti, R., Liang, X.H., Mizushima, N., Packer, M., Schneider, M.D., and Levine, B. (2005). Bcl-2 antiapoptotic proteins inhibit Beclin 1-dependent autophagy. Cell *122*, 927–939.

Pyo, J.O., Jang, M.H., Kwon, Y.K., Lee, H.J., Jun, J.I., Woo, H.N., Cho, D.H., Choi, B., Lee, H., Kim, J.H., et al. (2005). Essential roles of Atg5 and FADD in autophagic cell death: dissection of autophagic cell death into vacuole formation and cell death. J. Biol. Chem. *280*, 20722–20729.

Radoshevich, L., Murrow, L., Chen, N., Fernandez, E., Roy, S., Fung, C., and Debnath, J. (2010). ATG12 conjugation to ATG3 regulates mitochondrial homeostasis and cell death. Cell *142*, 590–600.

Schwartz, L.M., Smith, S.W., Jones, M.E., and Osborne, B.A. (1993). Do all programmed cell deaths occur via apoptosis? Proc. Natl. Acad. Sci. USA *90*, 980–984.

Sinha, S., and Levine, B. (2008). The autophagy effector Beclin 1: a novel BH3-only protein. Oncogene *27* (*Suppl 1*), S137–S148.

Suzuki, N.N., Yoshimoto, K., Fujioka, Y., Ohsumi, Y., and Inagaki, F. (2005). The crystal structure of plant ATG12 and its biological implication in autophagy. Autophagy *1*, 119–126.

Tanida, I., Ueno, T., and Kominami, E. (2004). LC3 conjugation system in mammalian autophagy. Int. J. Biochem. Cell Biol. *36*, 2503–2518.

Willis, S.N., and Adams, J.M. (2005). Life in the balance: how BH3-only proteins induce apoptosis. Curr. Opin. Cell Biol. *17*, 617–625.

Yang, Z., and Klionsky, D.J. (2010). Mammalian autophagy: core molecular machinery and signaling regulation. Curr. Opin. Cell Biol. *22*, 124–131.

Yin, X.M., Oltvai, Z.N., and Korsmeyer, S.J. (1994). BH1 and BH2 domains of Bcl-2 are required for inhibition of apoptosis and heterodimerization with Bax. Nature *369*, 321–323.

Yin, X., Cao, L., Kang, R., Yang, M., Wang, Z., Peng, Y., Tan, Y., Liu, L., Xie, M., Zhao, Y., et al. (2011). UV irradiation resistance-associated gene suppresses apoptosis by interfering with BAX activation. EMBO Rep. *12*, 727–734.

Yousefi, S., Perozzo, R., Schmid, I., Ziemiecki, A., Schaffner, T., Scapozza, L., Brunner, T., and Simon, H.U. (2006). Calpain-mediated cleavage of Atg5 switches autophagy to apoptosis. Nat. Cell Biol. *8*, 1124–1132.

Zalckvar, E., Yosef, N., Reef, S., Ber, Y., Rubinstein, A.D., Mor, I., Sharan, R., Ruppin, E., and Kimchi, A. (2010). A systems level strategy for analyzing the cell death network: implication in exploring the apoptosis/autophagy connection. Cell Death Differ. *17*, 1244–1253.

Zhu, Y., Zhao, L., Liu, L., Gao, P., Tian, W., Wang, X., Jin, H., Xu, H., and Chen, Q. (2010). Beclin 1 cleavage by caspase-3 inactivates autophagy and promotes apoptosis. Protein Cell *1*, 468–477.